



UNIVERSITY OF LEEDS

This is a repository copy of *A multi-dimensional analysis of pro-glacial landscape change at Sólheimajökull, Southern Iceland*.

White Rose Research Online URL for this paper:
<http://eprints.whiterose.ac.uk/87567/>

Version: Accepted Version

Article:

Staines, KEH, Carrivick, JL, Tweed, FS et al. (4 more authors) (2015) A multi-dimensional analysis of pro-glacial landscape change at Sólheimajökull, Southern Iceland. *Earth Surface Processes and Landforms*, 40 (6). 809 - 822. ISSN 0197-9337

<https://doi.org/10.1002/esp.3662>

Reuse

Unless indicated otherwise, fulltext items are protected by copyright with all rights reserved. The copyright exception in section 29 of the Copyright, Designs and Patents Act 1988 allows the making of a single copy solely for the purpose of non-commercial research or private study within the limits of fair dealing. The publisher or other rights-holder may allow further reproduction and re-use of this version - refer to the White Rose Research Online record for this item. Where records identify the publisher as the copyright holder, users can verify any specific terms of use on the publisher's website.

Takedown

If you consider content in White Rose Research Online to be in breach of UK law, please notify us by emailing eprints@whiterose.ac.uk including the URL of the record and the reason for the withdrawal request.



eprints@whiterose.ac.uk
<https://eprints.whiterose.ac.uk/>

A multi-dimensional analysis of proglacial landscape change at Sólheimajökull, southern Iceland

Kate E.H. Staines¹, Jonathan L. Carrivick¹ Fiona S. Tweed²,
Andrew J. Evans¹, Andrew J. Russell³, Tómas Jóhannesson⁴, Matthew Roberts⁴

¹School of Geography, University of Leeds, Woodhouse Lane, Leeds, West Yorkshire, LS2 9JT, UK.

²Geography, Staffordshire University, Science Centre, Leek Road, Stoke-on-Trent, ST4 2DF, UK

³School of Geography, Politics and Sociology, Faculty of Humanities and Social Sciences, Newcastle University, Newcastle upon Tyne, NE1 7RU, UK.

⁴Icelandic Meteorological Office, Bústaðavegi 9, 150 Reykjavík, Iceland

Correspondence to:

Dr. Jonathan Carrivick,

Email: j.l.carrivick@leeds.ac.uk

Tel.: 0113 343 3324

Abstract

Proglacial landscapes are some of the most active on Earth. Previous studies of proglacial landscape change have often been restricted to considering either sedimentological, geomorphological or topographic parameters in isolation and are often mono-dimensional. This study utilised field surveys and digital elevation model analyses to quantify planform, elevation and volumetric proglacial landscape change at Sólheimajökull in southern Iceland for multiple time periods spanning from 1960 to 2010. As expected, the most intense geomorphological changes persistently occurred in the ice-proximal area. During 1960 to 1996 the proglacial river was relatively stable. However, after 2001 braiding intensity was higher, channel slope shallower and there was a shift from overall incision to aggradation. Attributing these proglacial river channel changes to the 1999 jökulhlaup is ambiguous because it coincided with a switch from a period of glacier advance to that of glacier retreat. Furthermore, glacier retreat (of $\sim 40 \text{ m.yr}^{-1}$) coincided with ice-marginal lake development and these two factors have both altered the proglacial river channel head elevation. From 2001 to 2010 progressive increase in channel braiding and progressive downstream incision occurred; these together probably reflecting stream power due to increased glacier ablation and reduced sediment supply due to trapping of sediment by the developing ice-marginal lake. Overall, this study highlights rapid spatiotemporal proglacial landscape reactions to changes in glacial meltwater runoff regimes, glacier terminus position, sediment supply and episodic events such as jökulhlaups. Recognising the interplay of these controlling factors on proglacial landscapes will be important for understanding the geological record and for landscape stability assessments.

Keywords DEM; photogrammetry; LiDAR; sediment; moraine; glacier; river

38 **Introduction**

39 Proglacial landscapes are amongst the most dynamic on earth and are characterised by spatially and
40 temporally variable sediment and water fluxes (Maizels, 1979; Ashworth and Ferguson, 1986; Russell and
41 Marren, 1999; Marren, 2005; Carrivick and Rushmer, 2009). These variable fluxes are partly manifest in
42 proglacial river planform, elevation and volumetric changes. On a decadal scale, proglacial rivers can be
43 controlled by (i) climatically-driven glacier advance and retreat and hence glacier terminus elevation, (ii)
44 glacier mass balance, meltwater generation rates and volumes and hence river competence and capacity, (iii)
45 sediment supply, (iv) episodic events such as glacier outburst floods or ‘jökulhlaups’, and (v) base level
46 changes. The relative importance of these controls differ through time and they may interact, so consequently
47 proglacial landforms and deposits vary greatly, as do rates and patterns of landscape change (Marren, 2002a).
48 Understanding decadal-scale proglacial river changes has important implications for deciphering the
49 geological record and for assessments of landscape stability.

50 Prevailing models of proglacial landscape development are largely qualitative, e.g. sedimentology (Maizels,
51 1997), proglacial river network patterns (Gurnell et al., 2000), land systems (Evans and Twigg, 2002).
52 Quantitative studies of proglacial landscape development (e.g. ESP&L special issue on ‘Quantifying rates and
53 processes of landscape evolution, November 2011) must make repeated and precise measurement of the land
54 surface. Repeat surveys in proglacial areas are often focused on a particular component; for example on
55 braided rivers (e.g. Schiefer and Gilbert, 2007; Milan et al., 2007) or moraine evolution (e.g. Sletten et al.,
56 2001; Lyså and Lonne, 2001; Schomacker and Kjaer, 2007). In contrast, when whole proglacial areas are
57 assessed for sediment redistribution (e.g. Irvine-Fynn et al., 2011; Bennett and Evans (2012); Carrivick et al.
58 (2013a) sources and sinks can be identified and linkages and feedbacks established.

59 Previous surveys on proglacial rivers have often been mono-dimensional; i.e. river cross sections or long
60 profiles (e.g. Ashworth and Ferguson, 1986; Maizels, 1997; Marren, 2002a, 2005). Although terrestrial laser
61 scanning (TLS) and airborne light detection and ranging surveys (LiDAR) are now increasingly used in
62 proglacial geomorphological analyses (e.g. Magilligan et al., 2002; Milan et al., 2007; Carrivick et al., 2013a;
63 Williams et al., 2013), they trade better spatial resolution and 3D accuracy with limited temporal coverage.
64 Therefore, the studies on proglacial landscape evolution at Breiðamerkurjökull by Evans and Twigg (2002), at
65 Kvíárjökull, Iceland by Bennett and Evans (2012) and in the upper Lillooet Valley, British Columbia by
66 Schiefer and Gilbert (2007) are notable for spanning 100, 60 and 50 years, respectively.

67 Braided river morphology is often investigated through repeated planform studies (e.g. Brasington et al.,
68 2000), which can provide valuable information on lateral channel change, such as bar migration and bank

69 erosion. However, where information on elevation and volumetric change is lacking, channel form can be
70 misrepresented and geomorphic processes overlooked. The few studies that have focussed on elevation and
71 volume changes have quantified geomorphic processes; for example, Lane et al., (2003) used synoptic remote
72 sensing to estimate erosion and deposition volumes in a gravel-bedded braided river. Quantification of 3D
73 landscape change requires consistent, high-resolution (spatial and temporal) landscape datasets (Schneeberger
74 et al., 2007) which are rare. Where such datasets do exist, it is usually photogrammetric techniques that have
75 been employed; examples of such techniques being applied to the evolution of glacial landscapes include
76 Etzelmuller and Sollid (1997), Fox and Cziferszky (2008) and Bennett and Evans (2012). Deriving DEMs
77 photogrammetrically works well in ice-marginal and proglacial settings because of (i) a lack of vegetation, (ii)
78 highly textured surfaces, and (iii) the magnitude of geomorphological change, which is often considerably
79 greater than DEM uncertainty (Schiefer and Gilbert, 2007). Confidence in quantifying geomorphological
80 change between sequential DEMs is likely to be greater where this so-called ‘signal-to-noise ratio’ (James et
81 al., 2012) is high; i.e. where uncertainty is low. Multi-temporal landscape measurements can be used to
82 quantify rates of change and assess spatiotemporal variations in geomorphic processes; to-date this has been
83 achieved to a certain extent at a decadal scale (Schiefer and Gilbert, 2007; Bennett and Evans, 2012), but more
84 often on an inter-seasonal scale (e.g. Magilligan et al., 2002; Milan et al., 2007; Williams et al., 2013;
85 Carrivick et al., 2013a).

86 The aims of this study are to; (i) quantify multi-dimensional proglacial landscape change, (ii) evaluate the key
87 controls on this proglacial landscape change.

88 **Study area**

89 Sólheimajökull is an 8 km long outlet glacier of the Mýrdalsjökull ice cap in southern Iceland (
90 **Figure 1**). It is ~ 15 km long, has an area of ~ 47 km², a mean thickness of 270 m and an elevation range of
91 110 m.asl to 1450 m.asl Sigurdsson et al., (2007). The Jökulsá á Sólheimasandi river (abbreviated to Jökulsá)
92 flows southwards from the glacier terminus across Sólheimasandur and Skógasandur to the North Atlantic
93 Ocean over a distance of ~ 9 km. Streams join the Jökulsá from the Jökulsárgil and Fjallgil gorges to the west
94 and the Heiðarhorn valley to the east (

95 **Figure 1**). Sólheimajökull was selected as the study site for four reasons. Firstly, like other Icelandic glaciers,
96 Sólheimajökull and its proglacial area have been repeatedly photographed from the air since the mid-20th
97 Century and consequently repeat aerial photographs exist covering ~ 60 years. Secondly, Sólheimajökull has
98 one of the longest and most studied glacier fluctuation records in Iceland, extending back to the mid-Holocene

99 (Dugmore and Sugden 1991; Mackintosh et al., 2002; Casely and Dugmore, 2004) and the period of aerial
100 photograph coverage includes both glacier terminus advance and retreat phases. Thirdly, the sedimentology
101 and geomorphology of the proglacial area has also been intensely studied (e.g. Maizels 1989a, b, 1991, 1993,
102 1997), with the Holocene evolution of the sandur being relatively well-constrained. Fourthly, a glacier
103 outburst flood, or 'jökulhlaup', occurred in July 1999 at Sólheimajökull, offering the opportunity to examine
104 not only the impact of that event in comparison to ~30 years of preceding ice ablation-fed river flow, but also
105 the landscape response in the ~ 15 years afterwards.

106 Sólheimajökull is prone to jökulhlaups from the Katla volcanic system (Thorarinsson, 1975; Tweed, 2000).
107 The 1999 jökulhlaup produced several floodwater outlets at the glacier terminus and on the surface of the
108 glacier (Roberts et al., 2003). Peak discharge at the road bridge 4 km downstream of the glacier terminus was
109 calculated at $1700 \text{ m}^3 \text{ s}^{-1}$ and this was reached within an hour of flood onset (Sigurðsson et al, 2000). The river
110 is reported to have returned to normal flow conditions within a day (Sigurðsson et al., 2000; Russell et al.,
111 2010). There have been several analyses of the 1999 jökulhlaup event and the proglacial impacts were
112 extensive and are relatively well-understood (e.g. Roberts et al., 2000; Russell et al., 2000; Roberts et al.,
113 2003; Russell et al., 2010; Staines and Carrivick, this issue).

114 **Methodology**

115 Landscape change at Sólheimajökull from 1960 to 2010 was quantified through the analysis of a time-series
116 of orthophotographs and DEMs, in combination with field-surveying. Five sets of panchromatic black-and-
117 white stereo-pair aerial photographs (all those available in summer months); specifically in years 1960, 1975,
118 1984, 1990 and 1996, were obtained from Landmælingar Íslands (LMÍ). In 1975, 1990 and 1996, two parallel
119 flight lines were surveyed, producing four overlapping photographs for each of these years. In both 1960 and
120 1984 only one flight line was surveyed. Whilst the 1960 photographs cover the entire site, the lower 3 km of
121 the river channel were not surveyed in 1984. Each photograph on the flight-line overlaps by 60% with the next
122 image and by 30% between parallel flight-lines. The photographs were provided in digital format, having been
123 photogrammetrically scanned at 15 microns (1800 dpi) to give a ground pixel size of < 1 m (**Fig. 2A**). Colour
124 aerial orthophotographs of the Sólheimajökull terminus and Sólheimasandur for the years 2001 and 2009
125 were obtained from Loftmyndir ehf. (www.loftmyndir.is). These stereo-pair photographs were taken using a
126 metric (calibrated) frame camera and had been photogrammetrically processed by Loftmyndir ehf. to remove
127 image distortion. The colour orthophotographs were supplied as image files with a ground-pixel size of 50 cm.
128 LiDAR data at 2m grid resolution and < 0.1 m accuracy covering Sólheimajökull and the Jökulsá á
129 Sólheimasandi channel were obtained from the Icelandic Meteorological Office (Veðurstofa Íslands,

130 www.vedur.is), the survey having been conducted by Topscan GmbH (www.topscan.de) in summer 2010.

131 Orthophotographs for the years 1960 to 2009 were generated by georeferencing in Leica Photogrammetry
132 Suite (LPS) with knowledge of calibrated focal length, lens type and lens distortion (**Fig. 2**), and with 44
133 ground control points measured in the field with a Leica GPS500 dual phase differential global positioning
134 system (dGPS). The dGPS base station position was measured for 360 minutes and then post-processed
135 relative to the continuous active IGNS station at Höfn, yielding a 3D accuracy of 0.05 m. All GCPs were
136 surveyed relative to this base position in RTK mode and with accuracy of < 0.02 m. GCP positions are
137 indicated in **Figure 1** and sited at points that were (i) visible both in the field and on the aerial photographs,
138 (ii), immovable, features (Schiefer and Gilbert 2007) such as the corners of fields, the edges of buildings and
139 large, outsize boulders; (iii) visible in every set of photographs. As ground control could not be established
140 prior to the photograph surveys, this technique is ideal for the historical photograph analysis (Chandler 1999)
141 performed in this study. The GCPs were located in the ‘point measurement’ module of LPS (**Fig. 2C**) using
142 the automatic drive function, which automatically determines GCP location from the user-defined coordinates.
143 Triangulation errors were distributed across all of the images using a bundle block adjustment model (**Fig.**
144 **2D**). The addition of ‘advanced robust blunder checking’ significantly reduced the total image unit weight
145 RMSE; all values were smaller than 1 pixel (smaller than the original ground pixel size of the aerial imagery).

146 Topographic data were extracted in the LPS automatic terrain extraction (eATE) module (**Fig. 2E**) using the
147 default normalised cross correlation (NCC) reverse matching process with a 7 x 7 window size. Digital
148 Elevation Models (DEMs) (**Fig. 2F**) were generated at 2 m grid cell size resolution using the
149 photogrammetrically-extracted terrain points, photogrammetrically-extracted contours, airborne LiDAR data
150 and DGPS points. DEM quality and reliability is influenced by the method of data interpolation, but as
151 Schwendel et al., (2010) note, there is no preferred technique. To maximise the reliability and accuracy of the
152 photogrammetrically-derived DEMs, we interpolated a continuous surface through the input points with a
153 non-linear 5th-order polynomial Triangulated Irregular Network (TIN) technique (**Fig. 2F**); thus each input Z
154 value was honoured in the output surface to reduce error.

155 We do not have two DEMs produced independently of the same date. So to assess DEM uncertainty 482
156 points were sampled across the photogrammetrically-derived DEMs in areas of ‘stable’ terrain; i.e. non-
157 glacier and non-valley floor areas that we assumed had undergone little change over the period of study, using
158 the ‘Create Random Points’ ArcGIS tool. We made a quantitative comparison of the difference in elevation of
159 each of these points with the corresponding position in the LiDAR dataset. This comparison, which we
160 consider is the worst case scenario because in photogrammetrically-derived DEMs most error occurs on
161 steeper terrain, a heterogeneous difference in elevation; i.e. a DEM ‘error’, was revealed (c.f. Carlisle, 2005).

162 Inverse distance weighting interpolation between these spatially-distributed ‘error points’ generated an ‘error
163 surface’. This error surface was subtracted from each photogrammetrically-derived DEM to ‘correct’ the
164 photogrammetrically-derived DEM elevation values. Final photogrammetrically-derived DEM uncertainty
165 was quantified against dGPS points and 400 random points (different to those points used to identify error) in
166 the LiDAR dataset; mean elevation differences were 0.05 m and RMSE typically ~ 1.0 m (**Table 1**), both of
167 which are typical values for photogrammetrically-derived DEMs of proglacial areas (e.g. Evans and Twigg,
168 2002; Schiefer and Gilbert, 2002; Bennett and Evans, 2012). These RMSE values (**Table 1**) indicate the
169 uncertainty in elevation measurements. Assessment of uncertainty in our volume calculations follows that of
170 Lane et al. (2003) whereby we use ‘unthresholded’ DEMs of difference, because differences below the level
171 of detection are uncertain, and where volumetric uncertainty, \sum volume, is calculated as follows:

$$\sum \text{volume} = d^2 \sqrt{n} \sum DoD$$

172 where d is raster cell size, n is number of raster cells for which the DEM of difference is calculated, and
173 $\sum DoD$ is the error of the DEM of difference as given by $\sqrt{SD_DEM\#1^2 + SD_DEM\#2^2}$, where SD is the
174 standard deviation of residuals, displayed in **Table 1**. Volumetric uncertainties are reported in **Table 2** for the
175 DEM hillshaded in **Figure 3** and for valley floor areas as defined in perimeter by the steep river banks in the
176 2010 LiDAR data (**Fig. 3**).

177 Using the final orthophotographs and final DEMs, geomorphological maps were produced for each year of
178 this study in ArcGIS. Landforms were identified on the basis of their location, morphology, composition and
179 relationship with neighbouring features. Field surveying was conducted in the summers of 2009 and 2010 to
180 verify landform identification. To aid visualization, the corrected DEMs were visualized using multiple-
181 azimuth hill-shading (**Fig. 3**; Smith and Clark, 2005). A video animation of these hillshaded DEMs is
182 provided as supplementary information. The ice-proximal area was mapped in detail to generate data on
183 channel configuration patterns, features of ice-disintegration and stagnation, non-glacial deposits, the glacier
184 terminus and supraglacial features. Morphometric data were generated from the geomorphological maps,
185 DEMs and orthophotographs to quantitatively describe the landscape and calculate rates of geomorphological
186 change from 1960 to 2010. Elevation and volume data were also obtained from the DEMs to quantify
187 volumetric change over the study period. Spatially-distributed elevation and volume changes for each time
188 period were calculated by subtracting an earlier DEM surface from a later DEM so that negative values in
189 elevation change reflect a reduction in elevation over that time period. This was carried out for the first 6
190 reaches of the study area only, due to reduced DEM coverage in 1960, 1984 and 2009 (**Fig. 3**). It should also
191 be noted that quantification of glacier volume changes only applies to the mapped part of the glacier and not

192 to its entire extent.

193 Existing models of proglacial river channel network evolution (e.g. Gurnell et al., 2000) are largely
194 qualitative. This study quantified a series of metrics to define proglacial river channel evolution. The
195 proglacial area was split into 12 reaches (**Fig. 3**) to examine proximal to distal variability. Each of the 12
196 reaches were split into 10 cross-sections and the number of braids counted at each. These values were then
197 averaged to give a braid intensity value for each reach. Reach length was defined on the basis of the mean
198 wetted width (AWW), calculated by dividing the total wetted area (extracted from the digitised river channel)
199 by the length of the channel (measured along the thalweg of the largest channel). Egozi and Ashmore (2008)
200 proposed that reach length should be at least ten times the average wetted width (AWW) at mean daily
201 discharge; the largest AWW was measured in 2010, at 81 m. Reach length was therefore set at 810 m for each
202 year of study. Metrics to determine temporal changes between 1960 and 2010 included number of channels,
203 number of channel bars, thalweg length of main channel, sum of bar lengths, total length of all channels and
204 mean number of channel links and bar index (**Table 3**); all measured from 114 channel cross sections. Effects
205 of river stage varying in aerial photographs on these metrics were minimised by using the channel count index
206 (Egozi and Ashmore, 2008), which is the least sensitive to flow stage. The intensity of braiding along the
207 entire length of the Jökulsá was measured using Germanoski and Schumm's (1993) bar index (Equation 5,
208 page 60). We also measured the channel count index because it is not sensitive to variations in channel
209 sinuosity and orientation and has smallest coefficients of variation when compared to other braiding indices
210 (Egozi and Ashmore, 2008).

211 **Results**

212 Our results include qualitative observations and maps to give an overview of the landscape system, and
213 quantification of planform, length, elevation and volume changes on glacier and proglacial surfaces. Video
214 animations of some of these datasets and maps are provided as supplementary information. We firstly describe
215 the glacier changes (and have already given a brief summary of the 1999 jökulhlaup). Secondly, with these
216 two key controls on the proglacial area in mind, we describe the spatiotemporal pattern of proglacial
217 landscape changes.

218

219 **Glacier changes 1960 to 2010**

220 Sólheimajökull varied considerably in spatial extent between 1960 and 2010 (**Figure 4, 5, 6**), notably
221 temporarily blocking the tributary valley of Jökulsárgil (**Fig. 1**) at its largest extent during the 1980s and

222 1990s. Between 1960 and 1996, Sólheimajökull advanced approximately 400 m, increasing in area by 0.61
223 km² (Figs. 4A, 5, 6). During retreat, the glacier terminus position retreated by ~ 450 m and the (mapped) area
224 decreased by 74 %, from 1.11 km² in 1996 to 0.28 km² in 2010 (Figs. 5, 6). The rate of glacier length, glacier
225 area and glacier volume change was greatest in the time period 1996 to 2001, 2001 to 2009 and 1996 to 2001,
226 respectively (Figs. 6B and 6C). In 1960, 28 % of the glacier was debris-covered. The greatest proportion of
227 debris cover on the glacier terminus was in 2001; only 36 % of the mapped glacier area was categorised as
228 clear ice at this time when melt-out of englacial eskers and debris-rich ice bands, together with the elevation
229 of subglacial material to the terminus, resulted in the ice-marginal area of Sólheimajökull being characterised
230 by features of ice stagnation. However, by 2010 the percentage of the mapped glacier area that was debris-
231 covered had decreased to 15 %. In all years of study the aerial photographs indicate that the glacier surface
232 was heavily crevassed, and with debris-cones and debris ridges arranged both parallel and transverse to flow.
233 In 2009 and 2010 englacial debris-rich ice bands were visible in the field dipping up-glacier at the glacier
234 terminus, likely formed by the elevation of bed material from the subglacial overdeepening (e.g. Swift et al.,
235 2006), which is known to exist beneath Sólheimajökull (Mackintosh et al., 2000).

236 The surface elevation of the terminus of Sólheimajökull varied by up to 50 m between 1975 and 1984 (± 1.43
237 m) between each time period (Figure 7). Net elevation change from 1960 to 2010 was negative across the
238 glacier surface and in the immediate ice-proximal area. Glacier terminus advance and retreat caused changes
239 in the elevation of the (proglacial) channel head (Fig. 8A), although the measurement of this is probably an
240 underestimate due to the water surface of the ice-marginal lake being in the DEMs (see flat surface at 95 m.asl
241 in Fig. 7). In detail, for the time periods from 1960 to 1996, elevation change across the mapped area of the
242 glacier was positive (Fig. 7), indicating thickening of the glacier ice with its advance. Sólheimajökull terminus
243 volume increased by 0.078 km³ (± 0.024 km³) between 1960 and 1996. In contrast, elevation change across
244 the glacier was negative between 1996 to 2010 (Fig. 7), indicating thinning with ice terminus retreat. Glacier
245 volume decreased between 1996 and 2010 by 0.106 km³ (± 0.005 km³) (Fig. 6C).

246 **Proglacial changes 1960 to 2010**

247 The area covered by the glacier, hummocky and ice-cored moraine, push moraine, rivers, lakes and outwash
248 deposits is quantified in each year of study (Fig. 4). The total area of push moraine decreased by 0.06 km²
249 between 1960 and 2010. This change was most clearly visible at the northern end of the push-moraine belt
250 where Sólheimajökull advanced between 1960 and 1996 (Figure 5). The ice-marginal lake progressively
251 developed with ice terminus retreat after 1996 (Fig. 5). Erosion along the banks of the Jökulsá also resulted in
252 a reduction of the area of moraine (Figs. 4, 5). The largest area of hummocky moraine was recorded at 0.8
253 km² in both 1960 and 2001 (Fig. 4). No areas of hummocky moraine were identified in 1984 or 1990. A small

254 area of hummocky moraine was identified in the 1996 orthophotograph covering an area of 0.002 km².

255 Proglacial river channels exiting from the terminus of Sólheimajökull varied in position and number between
256 each mapped time-period (**Fig. 5**). In all years, the largest channel emerged from the northern side of the ice
257 terminus and was joined by smaller streams emerging from the centre and south of the terminus (**Figure 5**).
258 From the southern side of the glacier terminus, the proglacial channel flowed southwards and was braided for
259 much of its length (**Error! Reference source not found.5**). Approximately 2 km south of the glacier terminus,
260 flow within the Jökulsá was confined to a single thread channel for a distance of 1 km as it cut through a belt
261 of moraine (**Error! Reference source not found.**). This was the most steeply-incised section of the river,
262 after which the channel widened to a 1.5 km wide plain just north of the bridge. The moraine through which
263 the Jökulsá eroded (**Fig. 5**) is interpreted as push moraine. This is based on the saw-tooth, discontinuous
264 planform appearance of the ridges and their arrangement in a broad arc (e.g. Evans and Twigg, 2002; Evans et
265 al., 2007; Boulton, 1986). Low amplitude linear features aligned perpendicular to the moraine ridges are
266 considered to be fluted moraine (Evans and Twigg, 2002). The moraine ridges and fluted moraine are
267 persistent features over the period of this study (**Fig. 5**). This, together with the extensive vegetation cover and
268 position of the moraine above the active river channels, suggests that formation was pre-1960. The moraine,
269 along with some hillslopes, is a sediment source to the proglacial river as demonstrated by elevation
270 reductions interpreted to be due to erosion (**Fig. 5**). The impact of ice advance and retreat episodes and of the
271 1999 jökulhlaup can be identified visually in these maps (**Figs. 5**) and will be quantified in the next sections.

272 A net increase of 0.215 km² was measured in river channel area between 1960 and 2010 (**Fig. 4**) but this
273 statistic masks considerable spatiotemporal variability. Therefore a series of areal, vertical and volumetric
274 metrics were used to quantify the spatiotemporal configuration of the proglacial river channel (initiating from
275 the largest or northern outlet) through time (**Table 2 and Figs. 7, 9**). The area covered by the river channel
276 (was greatest in 2010, measuring 0.67 km², 7.5 % of the total mapped area (9.0 km²). The long profile of the
277 first 4.5 km of the proglacial channel varied little until the time period 1996 to 2001. Between 1996 and 2001
278 the river long profile became smoothed; minor hummocks were eroded and minor depressions were infilled
279 (**Fig. 7A**) and this is attributed to the morphodynamic processes of the 1999 jökulhlaup (Staines and
280 Carrivick, this issue). The number, area and length of river channel bars during glacier advance up to 1996
281 was statistically lower than during glacier retreat after 1996 (**Fig. 9A**). Bar area was well correlated with
282 wetted channel area ($R^2 = 0.9$). The area of river bars showed an overall increase from 1960 to 2010, from
283 0.56 to 0.76 km², and there were more bars after the 1999 jökulhlaup than before (**Fig. 9A**).

284 Mean proglacial river channel gradient has declined overall between 1960 and 2010 but there was a period of
285 steepening during 1975 to 1996; i.e. during glacier terminus advance (**Fig. 8B**). In absolute terms, the river

286 channel was steepest in 1960 and shallowest in 2009, measuring 0.012 m.m^{-1} and 0.009 respectively (**Fig. 8B**).
287 Reaches 1 and 2 showed the greatest variation in channel slope through time; the standard deviation of
288 channel slope in reach 1 was 0.012 m.m^{-1} , ten times greater than in reaches 8 to 12. The channel long profile
289 was relatively stable up until 1996 and varied most between 1996 and 2001 and between 2001 and 2010 (**Fig.**
290 **7**). In detail, **Figure 7**, which only shows the channel long profile in selected years for clarity, illustrates
291 infilling of minor depressions, subduing of minor hummocks and generally smoothing of the channel long
292 profile between 1996 and 2001; most likely due to the 1999 jökulhlaup (c.f. Staines and Carrivick, this
293 volume). Between 2001 and 2009, i.e. after the 1999 jökulhlaup, the channel long profile generally aggraded,
294 with elevation increases increasing in magnitude down channel (**Fig. 7**).

295 Braiding intensity calculated from the number of channel links varied both spatially and temporally (**Fig. 9B**).
296 Braiding intensities over the mapped area were generally higher in in the post-jökulhlaup/glacier retreat
297 period, ranging from 2.00 in 1996 to 3.37 in 2009 (**Table 3**). In 1975 and 1984, the mean number of channel
298 links ranged from 1.86 to 1.99 (**Table 3**). During glacier advance 1960 to 1996, the bar index value increased
299 by 1.2 in ice-proximal reaches (reaches 1 to 5) and decreased by up to 2 in ice-distal reaches (reaches 6 to 12)
300 (**Fig. 9C**). During glacier ice terminus retreat 1996 to 2010, the opposite occurred; bar index decreased in ice-
301 proximal reaches and increased in ice-distal reaches (**Fig. 9C**). Relatively, braiding intensity increased overall
302 by 39 % in 1996 to 2010 time period compared with the 1960 to 1996 time period. Notably, the change in
303 braiding intensity was greatest for a single time period between 1996 and 2001, which is the time period
304 including the 1999 jökulhlaup, and braiding intensity was the highest ever of the time studied herein
305 immediately following in 2001 and 2009 (**Table 3**).

306 Overall, elevation changes in the first six most proximal proglacial reaches (**Fig. 10**) produced volume
307 changes that were positive up until 1996 and negative from 1996 to 2010 (**Figure 10 inset graph**). Volume
308 changes calculated were ranging from $0.035 \text{ km}^3 (\pm 0.009 \text{ km}^3)$ between 1975 to 1984, to $-0.052 \text{ km}^3 (\pm 0.012$
309 $\text{km}^3)$ between 2001 and 2009 (**Figure 10 inset graph**). The relatively small change in volume from 2009 to
310 2010 is attributable to the small period of time. There was generally spatial incoherence in proglacial area up
311 to 1996 (**Fig. 10**), due in part to some random error in the photogrammetrically-derived DEMs. However, some
312 non-glacier and non-river channel contributions to changes in surface elevation in **Figure 10** can be
313 interpreted to be degradation of ice-cored moraine and at these points changes are typically at $\sim 0.2 \text{ m.yr}^{-1}$.
314 Some minor mass movements especially in fluvial gravel cliffs and on steep moraine ridge flanks are evident
315 and so is ice-marginal lake development coincident with glacier terminus break up and detachment (**Fig. 10**).

316 **Discussion**

317 The most noticeable landscape changes at Sólheimajökull between 1960 and 2010 have been the extent and
318 elevation of the glacier, the physical characteristics of the immediate ice-proximal area and the configuration
319 of the proglacial channel network. The quantifications presented herein (i) acknowledge the potential
320 uncertainty in the photogrammetrically-derived DEMs as a ‘noise’, (ii) permit a signal of elevation changes and
321 hence geomorphological activity to emerge, and thereby (iii) enable testing of a number of conceptual models
322 of controls on proglacial landscape evolution, particularly those concerning proglacial river channels.

323 **Glacier advance and retreat**

324 The historical glacier terminus advance and retreat pattern and the magnitude of these changes at
325 Sólheimajökull are typical of (non-surge type) glaciers in Iceland (c.f. Sigurdsson et al., 2007). Whilst the
326 1999 jökulhlaup occurred virtually at the same time as the switch from glacier advance to retreat phases, the
327 relationship, if any, between the two factors remains unclear. The rate of retreat of Sólheimajökull between
328 1930 and 1970 was 25 m.yr^{-1} (Mackintosh et al., 2002), which is substantially lower than between 1996 and
329 2010, where the Sólheimajökull terminus retreated on average 40 m.yr^{-1} (Fig. 7). Without ice surface velocity
330 data, understanding retreat, area and volume changes is difficult, but it is notable that whilst debris cover on
331 the terminus has decreased, the ice-marginal lake has developed and expanded (Fig. 5). Glacier length, area
332 and elevation and volume changes (Fig. 10) observations and calculations have important climatic
333 implications. Changes in the historical geometry of Sólheimajökull has been linked to changes in precipitation
334 and temperature fluctuations (Mackintosh et al., 2002). Sólheimajökull has a high mass balance gradient,
335 meaning that extensive changes can be expected with only relatively small mass balance variations
336 (Mackintosh et al., 2000). This sensitivity of the glacier to climate is manifest in the dynamic proglacial
337 landscape, as will be discussed in the next section. However, the inherent coupling between the glacier and
338 proglacial landscape has become complicated by development and expansion of an ice-marginal lake. Retreat
339 of the glacier terminus into ever deeper water due to a subglacial overdeepening could promote calving and
340 thermo-mechanical ice mass loss (Carrivick and Tweed, 2013) and thus accelerate the decline in ice mass
341 volume. Development of the ice-marginal lake will also buffer the meltwater and sediment supply from the
342 glacier to the proglacial landscape. If retreat continues at a similar rate to at present; 40 m.yr^{-1} , Sólheimajökull
343 will have retreated from the area covered by the geomorphological maps presented in this study within 17
344 years.

345 **Proglacial river channel configuration**

346 Quantification of changes in proglacial landscapes including ice-cored moraine degradation, river planform

347 and elevation changes, and rates of fluvial aggradation/incision and volumes of material transported in
348 proglacial landscapes are very rare. Major river planform changes are often observed during ice terminus
349 advance (Marren, 2002c, 2005). Braiding usually increases in ice-proximal positions during ice advance
350 because aggradation rates tend to be higher (Marren, 2002a, c). However, ice volume loss increases meltwater
351 generation and hence the competence of meltwater streams probably increases (Maizels, 1979). There are
352 therefore three general models of controls on proglacial fluvial systems; progradation of an existing
353 (equilibrium) long profile simply due to ice margin advance (c.f. Thompson and Jones, 1986), changes in
354 sediment supply (e.g. Germanoski and Schumm, 1993) or meltwater supply (Maizels, 1979). All these three
355 models support the most intense river changes being situated ice-proximally. At Sólheimajökull, whilst
356 channel long profile gradient has declined with recent ice terminus retreat (Figs. 8B, 9B), proximal to distal
357 variations in channel braiding (Fig. 9B) are apparently unrelated to the changes in channel slope. It is
358 suggested that these proglacial river planform changes were primarily a response to large-scale sediment
359 transport during the 1999 jökulhlaup and the development of an ice-marginal lake (Fig. 7). These two
360 controls; the 1999 jökulhlaup and the ice-marginal lake development, perhaps explain why the conceptual
361 model of Germanoski and Schumm (1993); where a reduction in sediment supply tends to encourage
362 degradation ice-proximally and aggradation downstream, is supported (Figs. 9B, 9C). Specifically, this study
363 found pronounced river channel incision in the post-jökulhlaup/glacier retreat phase (Fig. 7) and coincident
364 increased braiding. River incision implies a sediment supply limit either due to stream power as meltwater
365 from ice ablation increases, and/or due to trapping of sediment in the developing ice-marginal lake. Thus it
366 can be interpreted that sediment fluxes from channel banks, moraines, and slopes (Fig. 10) has been low in the
367 post-jökulhlaup/glacier retreat phase (c.f. Carrivick et al., 2013b). From 2001 to 2010 the progressive increase
368 in downstream channel braiding (Fig. 9B) suggests that sediment deposited by the jökulhlaup was moving
369 through the proglacial channel system. These interpretations of the spatial disparity in landscape response to
370 the 1999 jökulhlaup imply that jökulhlaup deposits in the geological record could be spatially heterogenous
371 and therefore challenging to recognise.

372 The impact of the 1999 jökulhlaup is further evident in Figure 11A where the maximum range of fluvial
373 activity is within the time period 1996 to 2001 and the only time period with aggradation in all distal reaches
374 is 1996 to 2001. At Sólheimajökull, proglacial fluvial incision rates of up to 0.53 m.yr^{-1} ($\pm 5.11 \text{ m.yr}^{-1}$)
375 occurred in 1960 to 1975 and aggradation rates of up to 0.17 m.yr^{-1} ($\pm 1.39 \text{ m.yr}^{-1}$) occurred in 1984 to 1990.
376 These fluvial incision rates correspond well with measurements at Svinafellsjökull by Thompson and Jones
377 (1986) and at Skaftefellsjökull by Marren (2002c) (Fig. 11B). However, it should firstly be noted that this is
378 the only study with measurements of aggradation rates (Fig. 11B). Secondly, there is a difference in the
379 typical observation interval within each study and it could be suggested that longer time intervals present

380 smaller amounts of measurable geomorphological activity (Fig. 11). Such a time interval bias was noted in a
381 study of alpine geomorphological activity by Carrivick et al. (2013a). Nonetheless, these time period biases
382 merely highlight the difference between gross and net activity; considerable re-working of sediment occurs
383 and this can serve to infill hollows and subdue hummocks, for example. The volume of material moved
384 fluvially, in the first 6 reaches (~ 4 km) in each time period (Fig. 9) is an order of magnitude greater than the
385 volume of material moved across a sandur and along a proglacial stream determined by differencing airborne
386 LiDAR DEMs by Irvine-Fynn et al. (2011) for a 8 km² proglacial area in Svalbard.

387 **Conclusions**

388 This study adds to the very limited quantitative database on decadal-scale proglacial landscape development,
389 explicitly providing planform, elevation and volumetric calculations discriminated by major landform
390 components. It has examined the association of these spatiotemporal changes with the major controls of
391 glacier terminus advance and retreat, a jökulhlaup and development of an ice-marginal lake. The main
392 conclusions discriminated by this study are:

- 393 1. Between 1960 and 1996, Sólheimajökull advanced ~ 23 m.yr⁻¹, whereas between 1996 and 2010
394 Sólheimajökull retreated at ~ 40 m.yr⁻¹; the fastest retreat recorded since historical records began. This
395 retreat rate is comparable to that at many other Arctic glaciers and they respond to atmospheric warming
396 and climate change. The greatest rate of change in glacier volume was observed between 1996 and 2001;
397 an average of -0.009 km³ yr⁻¹ (± 0.009 km³ yr⁻¹) coincidentally with the time of the 1999 jökulhlaup.
- 398 2. Proglacial fluvial incision rates of up to 0.53 m.yr⁻¹ (± 5.11 m.yr⁻¹) occurred in 1960 to 1975 and
399 aggradation rates of up to 0.17 m.yr⁻¹ (± 1.39 m.yr⁻¹) occurred in 1984 to 1990. Whilst noting the
400 uncertainty attached to these calculations, with caution these rates are considered to be higher than
401 measured at other southern Iceland glaciers. Proglacial volume changes were positive between 1960 to
402 1996 and up to 0.038 km³ (± 0.009 km³) between 1975 and 1984, and negative in the time period 1996 to
403 2010 and up to -0.051 km³ (± 0.005 km³) between 2001 and 2009. These volume changes are an order of
404 magnitude higher than measured on Svalbard by Irvine-Fynn et al (2011).
- 405 3. Spatially, the most rapid geomorphological changes persistently occurred ice-proximally. Temporally,
406 the most intense geomorphological changes occurred between 2001 and 2009. This is rather unexpected
407 because it the time period 1996 to 2001 is that which includes the 1999 jökulhlaup. However, the
408 landscape response to the 1999 jökulhlaup may be masked by; (i) the interval of time elapsed between
409 surveys in this study, (ii) the switch from glacier terminus advance to retreat and the development of an
410 ice-marginal lake.
- 411 4. The proglacial sandur and river channel long profile were relatively stable up until 1996 but the 1999

412 jökulhlaup smoothed the long profile considerably. Furthermore, the increase in channel braiding
413 intensity, decrease in channel slope and reach-based volume changes together indicated that sediment
414 supply decreased after 1996. Whether this change in the proglacial river was a reaction to the 1999
415 jökulhlaup, to a phase of glacier retreat or to the development of an ice-marginal lake remains unclear.

416 5. Proximally, the 1999 jökulhlaup had a clear and lasting depositional impact, with only minor reworking
417 and erosion of the ice-marginal deposits occurring in the decade since the flood. In contrast, distal
418 changes between 2001 and 2010 were characterised by progressive channel incision.

419 More widely, channel aggradation rates have implications for landscape management; for the viability of
420 road bridges and flood protection bunds, for example. In the future, retreat of the terminus into an
421 overdeepened basin and an enlarging ice-marginal lake could together mean that sediment supply to the
422 proglacial area decreases, resulting in a stabilisation of proglacial channel incision rates (e.g. Roussel et al.,
423 2008). Recognition of the interplay of factors controlling proglacial landscape development and the linkages
424 between components of the proglacial landscape has important implications for understanding the geological
425 record and for landscape management.

426 **Acknowledgements**

427 This research was funded by a NERC Doctoral training grant to KEH at the University of Leeds. Thanks to
428 Bjarney Guðbjörnsdóttir and Dalia Prizginiene at Landmælingar Íslands and Kristinn Sveinsson and Skúli
429 Þorvaldsson at Loftmyndir ehf. for their provision of data and helpful advice. Chris Williams, Katie Little,
430 Bernadette Barry and the 2009 Earthwatch team (Mary-Beth Aberlin, Noah Aberlin, Candic Autry and Frank
431 Macchi) are thanked for help with fieldwork. Rob Duller is thanked for useful discussions. Stuart Lane and
432 three anonymous reviewers are thanked for their expansive, critical yet very constructive comments.

433

434 **References**

- 435 Aðalgeirsdóttir, G., Guðmundsson, S., Björnsson, H., Pálsson, F., Jóhannesson, T., Hannesdóttir, H., Sigurðsson, S.,
436 Berthier, E. 2011. Modelling the 20th and 21st century evolution of Hoffellsjökull glacier, SE-Vatnajökull, Iceland.
437 *Cryosphere* **5**: 961-975.
- 438 Ashworth, P. J., Ferguson, R. I., 1986. Interrelationships of channel processes, changes and sediment in a proglacial
439 braided river. *Geografiska Annaler, Series A* **68**: 361-371.
- 440 Benn, D. I., Evans, D. J. A., 2010. *Glaciers and Glaciation*. Hodder Arnold, London.
- 441 Bennett, G. L., Evans, D. J. A., 2012, Glacier retreat and landform production on an overdeepened glacier foreland: the
442 debris-charged glacial landsystem at Kvíárjökull, Iceland. *Earth Surface Processes and Landforms* **37**: 1584–1602.
- 443 Boulton, G. S., 1986. Push-moraines and glacier-contact fans in marine and terrestrial environments. *Sedimentology*
444 **33**:677–698.
- 445 Brasington, J., Rumsby, B. T., McVey, R. A., 2000. Monitoring and modelling morphological change in a braided
446 gravel-bed river using high resolution GPS-based survey. *Earth Surface Processes and Landforms* **25**: 973-990.
- 447 Burke, M. J., Woodward, J., Russell, A. J., Fleisher, P. J., 2009. Structural controls on englacial esker sedimentation:
448 Skeiðarárjökull, Iceland. *Annals of Glaciology* **50**: 85-92.
- 449 Carlisle, B. H., 2005. Modelling the spatial distribution of DEM error. *Transactions in GIS* **9**: 521-540.
- 450 Carrivick, J. L., Rushmer, E. L., 2009. Inter- and intra-catchment variations in proglacial geomorphology: An Example
451 from Franz Josef Glacier and Fox Glacier, New Zealand. *Arctic, Antarctic and Alpine Research* **41**: 18-36.
- 452 Carrivick, J.L., Tweed, F.S., 2013. Proglacial lakes: character, behaviour and geological importance. *Quaternary Science*
453 *Reviews* **78**: 34–52.
- 454 Carrivick, J.L., Geilhausen, M., Warburton, J., Dickson, N.E., Carver, S.J., Evans, A.E., Brown, L.E., 2013a.
455 Contemporary geomorphological activity throughout the proglacial area of an alpine catchment. *Geomorphology* **188**:
456 83-95.
- 457 Carrivick, J.L., Turner, A.G.D., Russell, A.J., Ingeman-Nielsen, T., Yde, J.C., 2013b. Outburst flood evolution at Russell
458 Glacier, western Greenland: effects of a bedrock channel cascade with intermediary lakes. *Quaternary Science Reviews*
459 **67**: 39–58.
- 460 Casely, A. F., Dugmore, A. J., 2004. Climate change and 'anomalous' glacier fluctuations: the southwest outlets of
461 Mýrdalsjökull, Iceland. *Boreas* **33**: 108-122.
- 462 Dowdeswell, J. A., Ove Hagen, J., Björnsson, H., Glazovsky, A. F., Harrison, W. D., Holmlund, P., Jania, J., Koerner, R.
463 M., Lefauconnier, B., Ommanney, C. S. L., Thomas., R. H., 1997. The mass balance of circum-Arctic glaciers and recent
464 climate change. *Quaternary Research* **48**: 1-14.
- 465 Dugmore, A. J., Sugden, D. E., 1991. Do the anomalous fluctuations of Sólheimajökull reflect ice-divide migration?
466 *Boreas* **20**: 105-113.
- 467 Egozi, R., Ashmore, P., 2008. Defining and measuring braiding intensity. *Earth Surface Processes and Landforms* **33**:
468 2121-2138.
- 469 Etzelmüller, B., Sollid, J.L. 1997. Glacier geomorphometry - an approach for analyzing long-term glacier surface

- 470 changes using grid-based digital elevation models. *Annals of Glaciology* **24**: 135-141.
- 471 Evans, D. J. A., Twigg, D. R., 2002. The active temperate glacial landsystem: a model based on Breiðamerkurjökull and
472 Fjallsjökull, Iceland. *Quaternary Science Reviews* **21**: 2143-2177.
- 473 Evans, D. J. A., Twigg, D. R., Rea, B. R., Shand, M., 2007. Surficial geology and geomorphology of the Brúarjökull
474 surging glacier landsystem. *Journal of Maps* **2007**: 349-367.
- 475 Fox, A. J., Cziferszky, A., 2008. Unlocking the time capsule of historic aerial photography to measure changes in
476 Antarctic Peninsula glaciers. *Photogrammetric Record* **23**: 51-68.
- 477 Frey, H., Haerberli, W., Linsbauer, A., Huggel, C., Paul, F., 2010. A multi-level strategy for anticipating future glacier
478 lake formation and associated hazard potentials. *Natural Hazards and Earth System Sciences* **10**: 339-352.
- 479 Germanoski, D., Schumm, S. A., 1993. Changes in braided river morphology resulting from aggradation and
480 degradation. *Journal of Geology* **101**: 451-466.
- 481 Gurnell, A. M., Edwards, P. J., Petts, G. E., Ward, J. V., 2000. A conceptual model for alpine proglacial river channel
482 evolution under changing climatic conditions. *Catena* **38**: 223-242.
- 483 Hopkinson, C., Hayashi, M., Peddle, D., 2009. Comparing alpine watershed attributes from LiDAR, Photogrammetric
484 and Contour-based Digital Elevation Models. *Hydrological Processes* **23**: 451-463.
- 485 Huggel, C., Kaab, A., Haerberli, W., Teysseire, P., Paul, F., 2002. Remote sensing based assessment of hazards from
486 glacier lake outbursts: a case study in the Swiss Alps. *Canadian Geotechnical Journal* **39**: 316-330.
- 487 Irvine-Fynn, T.D.L., Barrand, N.E., Porter, P.R., Hodson, A.J., Murray, T., 2011. Recent High-Arctic glacial sediment
488 redistribution: A process perspective using airborne lidar. *Geomorphology* **125**: 27-39.
- 489 James, L. A., Hodgson, M. E., Ghoshal, S., Latiolais, M. M., 2012. Geomorphic change detection using historic maps
490 and DEM differencing: The temporal dimension of geospatial analysis. *Geomorphology* **137**: 181-198.
- 491 Koul, M. N., Ganjoo, R. K., 2010. Impact of inter- and intra-annual variation in weather parameters on mass balance and
492 equilibrium line altitude of Naradu Glacier (Himachal Pradesh), NW Himalaya, India. *Climatic Change* **99**: 119-139.
- 493 Lane, S.N., Westaway, R.M., Hicks, D.M. 2003. Estimation of erosion and deposition volumes in a large, gravel-bed,
494 braided river using synoptic remote sensing. *Earth Surface Processes and Landforms* **28**: 249-271.
- 495 Lyså, A., Lonne, I. 2001: Moraine development at a small High-Arctic valley glacier: Rieperbreen, Svalbard. *Journal of*
496 *Quaternary Science* **16**: 519-529.
- 497 Mackintosh, A. N., Dugmore, A. J., Hubbard, A. L., 2002. Holocene climatic changes in Iceland: evidence from
498 modelling glacier length fluctuations at Solheimajökull: *Quaternary International* **91**: 39-52.
- 499 Mackintosh, A. N., Dugmore, A. J., Jacobsen, F. M., 2000. Ice-thickness measurements on Sólheimajökull, southern
500 Iceland and their relevance to its recent behaviour. *Jökull* **48**: 9-16.
- 501 Magilligan, F. J., Gomez, B., Mertes, L. A. K., Smith, L. C., Smith, N. D., Finnegan, D., Garvin, J. B., 2002.
502 Geomorphic effectiveness, sandur development, and the pattern of landscape response during jökulhlaups:
503 Skeiðarársandur, southeastern Iceland. *Geomorphology* **44**: 95-113.
- 504 Magnusson, E., Björnsson, H., Dall, J., Pálsson, F., 2005. The 20th century retreat of ice caps in Iceland derived from
505 airborne SAR: W-Vatnajökull and N-Myrdalsjökull. *Earth and Planetary Science Letters* **237**: 508-515.

- 506 Maizels, J., 1979. Proglacial aggradation and changes in braided channel patterns during a period of glacier advance: An
507 Alpine example: *Geografiska Annaler Series A* **61**: 87-101.
- 508 -, 1989a. Sedimentology and palaeohydrology of Holocene flood deposits in front of a jokulhlaup glacier, south Iceland,
509 in Bevan, K., and Carling, P. A., eds., *Floods: Hydrological, Sedimentological and Geomorphological Implications*. John
510 Wiley and Sons Chichester, UK 239-251.
- 511 -, 1989b. Sedimentology, Paleoflow Dynamics and Flood History of Jokulhlaup Deposits - Paleohydrology of Holocene
512 Sediment Sequences in Southern Iceland Sandur Deposits. *Journal of Sedimentary Petrology* **59**: 204-223.
- 513 -, 1991. The origin and evolution of Holocene sandur deposits in areas of jokulhlaup drainage, Iceland, in Maizels, J., and
514 Caseldine, C., eds., *Environmental Change in Iceland: Past and Present*. Kluwer Academic Publishers, Netherlands 267-
515 302.
- 516 -, 1993. Lithofacies variations within sandur deposits: the role of runoff regime, flow dynamics and sediment supply
517 characteristics. *Sedimentary Geology* **85**: 229-325.
- 518 -, 1997. Jökulhlaup deposits in proglacial areas. *Quaternary Science Reviews* **16**: 793-819.
- 519 Marren, P. M., Toomath, S. C., 2012. Fluvial adjustments in response to glacier retreat: Skaftafellsjökull, Iceland. *Boreas*
520 **42**: 57-70.
- 521 Marren, P. M., 2002a. Criteria for distinguishing high magnitude flood events in the proglacial fluvial sedimentary
522 record: The Extremes of the Extremes: Extraordinary Floods (Proceedings of a symposium held at Reykjavik, Iceland,
523 July 2000) IAHS Publ. **271**.
- 524 -, 2002b. Fluvial-lacustrine interaction on Skeiðarársandur, Iceland: implications for sandur evolution. *Sedimentary*
525 *Geology* **149**: 43-58.
- 526 -, 2002c. Glacier margin fluctuations, Skaftafellsjökull, Iceland: implications for sandur evolution. *Boreas* **31**: 75-81.
- 527 -, 2005. Magnitude and frequency in proglacial rivers: a geomorphological and sedimentological perspective. *Earth-*
528 *Science Reviews* **70**: 203-251.
- 529 Milan, D. J., Heritage, G. L., Hetherington, D., 2007. Application of a 3D laser scanner in the assessment of erosion and
530 deposition volumes and channel change in a proglacial river. *Earth Surface Processes and Landforms* **32**: 1657-1674.
- 531 Roberts, M.J., Russell, A.J., Tweed, F.S., Knudsen, Ó., 2000. Ice fracturing during jökulhlaups: implications for
532 englacial floodwater routing and outlet development. *Earth Surface Processes and Landforms* **25**: 1429-1446.
- 533 Roberts, M.J., Tweed, F.S., Russell, A.J., Knudsen, Ó., Harris, T.D. 2003. Hydrologic and geomorphic effects of
534 temporary ice-dammed lake formation during jökulhlaups. *Earth Surface Processes and Landforms* **28**: 723-737.
- 535 Roussel, E., Chenet, M., Grancher, D., Jomelli, V., 2008. Processes and rates of post-Little Ice Age proximal sandar
536 incision (southern Iceland). *Geomorphologie-Relief Processus Environnement* **4**: 235-247.
- 537 Russell, A. J., Marren, P. M., 1999. Proglacial fluvial sedimentary sequences in Greenland and Iceland: A case study
538 from active proglacial environments subject to jökulhlaups, in Jones, A. P., Tucker, M. E., and Hart, J., eds., *The*
539 *Description and Analysis of Quaternary Stratigraphic Field Sections*. Quaternary Research Association, London.
- 540 Russell, A. J., Tweed, F. S., Knudsen, Ó., 2000. Flash flood at Sólheimajökull heralds the reawakening of an Icelandic
541 subglacial volcano. *Geology Today* **16**: 102-106.
- 542 Russell, A. J., Knudsen, O., Fay, H., Marren, P. M., Heinz, J., Tronicke, J., 2001. Morphology and sedimentology of a

- 543 giant supraglacial, ice-walled, jokulhlaup channel, Skeiðararjökull, Iceland: implications for esker genesis. *Global and*
544 *Planetary Change* **28**: 193-216.
- 545 Russell, A. J., Tweed, F. S., Roberts, M. J., Harris, T. D., Guðmundsson, M. T., Knudsen, Ó., Marren, P. M., 2010. An
546 unusual jökulhlaup resulting from subglacial volcanism, Sólheimajökull, Iceland. *Quaternary Science Reviews* **29**: 1363-
547 1381.
- 548 Schiefer, E., Gilbert, R., 2007. Reconstructing morphometric change in a proglacial landscape using historical aerial
549 photography and automated DEM generation: *Geomorphology* **88**: 167-178.
- 550 Schneeberger, N., Buergi, M., Hersperger, A. M., Ewald, K. C., 2007. Driving forces and rates of landscape change as a
551 promising combination for landscape change research - An application on the northern fringe of the Swiss Alps: *Land*
552 *Use Policy* **24**: 349-361.
- 553 Schomacker, A., Kjær, K. 2007. Origin and de-icing of multiple generations of ice-cored moraines at Brúarjökull,
554 Iceland. *Boreas* **36**: 411-425.
- 555 Schwendel, A. C., Fuller, I. C., Death, R. G., 2012. Assessing DEM interpolation methods for effective representation of
556 upland stream morphology for rapid appraisal of bed stability. *River Research and Applications* **28**: 567-584.
- 557 Sigurðsson, O., Zóphóníasson, S., Ísleifsson, E., 2000. Jökulhlaup úr Sólheimajökuli 18 Júlí 1999. *Jökull* **49**: 75-80.
- 558 Sigurdsson, O., Jonsson, T., Johannesson, T., 2007. Relation between glacier-termini variations and summer temperature
559 in Iceland since 1930. *Annals of Glaciology* **46**, 170-176.
- 560 Sletten, K., Lyså, A., Lønne, I., 2001. Formation and disintegration of a high-arctic ice-cored moraine complex, Scott
561 Turnerbreen, Svalbard. *Boreas* **30**: 272-284
- 562 Smith, M. J., Clark, C. D., 2005. Methods for the visualization of digital elevation models for landform mapping: *Earth*
563 *Surface Processes and Landforms* **30**: 885-900.
- 564 Swift, D.A., Evans, D.J.A., Fallick, A., 2006. Transverse englacial debris-rich ice bands at Kviárjökull, southeast Iceland.
565 *Quaternary Science Reviews* **25**: 1708-1718.
- 566 Thorarinsson, S. 1975. *Katla og annáll Kötlugosa. Árbók Ferðafélags Íslands*. Reykjavík: 125-149.
- 567 Thompson, A., Jones, A., 1986. Rates and causes of proglacial river terrace formation in southeast Iceland: an application
568 of lichenometric dating techniques. *Boreas* **15**: 231-246.
- 569 Tweed, F.S., 2000. An ice-dammed lake in Jökulsárgil: predictive modeling and geomorphological evidence. *Jökull* **48**:
570 17-28.
- 571 Westaway, R. M., Lane, S. N., Hicks, D. M., 2000. The development of an automated correction procedure for digital
572 photogrammetry for the study of wide, shallow, gravel-bed rivers. *Earth Surface Processes and Landforms* **25**: 209-226.
- 573 Williams, R. D., Brasington, J., Vericat, D., Hicks, D. M., 2013. Hyperscale terrain modelling of braided rivers: fusing
574 mobile terrestrial laser scanning and optical bathymetric mapping: *Earth Surface Processes and Landforms* **39**: 167-183.
- 575

576 A multi-dimensional analysis of proglacial landscape
 577 change at Sólheimajökull, southern Iceland

578 Kate E.H. Staines, Jonathan L. Carrivick, Fiona S. Tweed, Andrew J. Evans, Andrew J. Russell, Tómas
 579 Jóhannesson, Matthew Roberts
 580

		1960	1975	1984	1990	1996	2001	2009
Mean dZ (m)	Before	2.11	-0.07	0.12	-0.07	1.07	-0.16	0.09
	After	-0.04	-0.02	-0.01	-0.01	-0.03	0.002	0.001
Standard deviation dZ	Before	11.26	2.18	1.19	2.52	1.27	1.27	2.28
	After	4.91	1.44	0.97	0.99	0.89	1.24	2.25
RMSE dZ	Before	11.44	2.18	1.19	2.52	1.66	1.29	2.28
	After	4.91	1.43	0.97	0.99	0.89	1.24	2.25

581

582 Table 1: Assessment of digital elevation model error at 482 random points before and after correction using
 583 derivation of a spatially-variable 'error surface'. dZ is the elevation difference of all grid cells between a
 584 photogrammetrically-derived DEM and the LiDAR-derived DEM.
 585

586

587

588

589

590

591

592

593

594

595

596 A multi-dimensional analysis of proglacial landscape
 597 change at Sólheimajökull, southern Iceland

598 Kate E.H. Staines, Jonathan L. Carrivick, Fiona S. Tweed, Andrew J. Evans, Andrew J. Russell, Tómas
 599 Jóhannesson, Matthew Roberts

600

601 A

year	area (km ²)		count of cells, n		elevation	Uncertainty all DEM (km ³)	Uncertainty valley floor (km ³)
	all DEM	valley floor	all DEM	valley floor	SD dZ (m)		
1960	5.7	2.5	1425000	625000	4.91	0.023	0.016
1975	9	4.7	2250000	1175000	1.43	0.009	0.006
1984	6.3	2.6	1575000	650000	0.97	0.005	0.003
1990	9	4.6	2250000	1150000	0.99	0.006	0.004
1996	9	4.5	2250000	1125000	0.89	0.005	0.004
2001	9	4.7	2250000	1175000	1.24	0.007	0.005
2009	5.1	2.4	1275000	600000	2.25	0.010	0.007
2010	23.5	6.3	5875000	1575000	(baseline from which error assessed)		

602

603

B

	SigmaDoD (m)	Uncertainty (km ³)
1960 to 1975	5.11	0.024
1975 to 1984	1.73	0.009
1984 to 1990	1.39	0.007
1990 to 1996	1.33	0.008
1996 to 2001	1.53	0.009
2001 to 2009	2.57	0.012
1960 to 1996	4.99	0.024
1996 to 2001	1.53	0.009
1996 to 2010	0.89	0.005

604 Table 2: Propagation of error as defined by standard deviation (SD) in elevation measurements in Table 1 to
 605 uncertainty in volume calculations (part A) and change in volume calculations for time periods reported in this
 606 study (part B). DEM area in A is that hillshaded in Figure 3.

607

608 A multi-dimensional analysis of proglacial landscape
609 change at Sólheimajökull, southern Iceland

610 Kate E.H. Staines, Jonathan L. Carrivick, Fiona S. Tweed, Andrew J. Evans, Andrew J. Russell, Tómas
611 Jóhannesson, Matthew Roberts
612

613

Year	Total Number of Bars	Centre-line Length of Main Channel (km)	Sum of Bar Lengths (km)	Total length of all channels (km)	Mean number of channel links*	Bar index
1960	119	10.1	13.3	29.1	2.4	3.0
1975	77	10.3	8.2	21.7	1.9	1.9
1984	60	6.5	6.3	15.4	1.9	2.2
1990	204	9.9	15.3	32.3	2.7	3.4
1996	145	9.7	9.2	23.3	2.0	2.0
2001	341	10.2	21.5	40.5	3.3	4.7
2009	231	10.3	21.9	42.4	3.4	4.8
2010	124	10.6	16.9	34.0	2.9	3.5

614

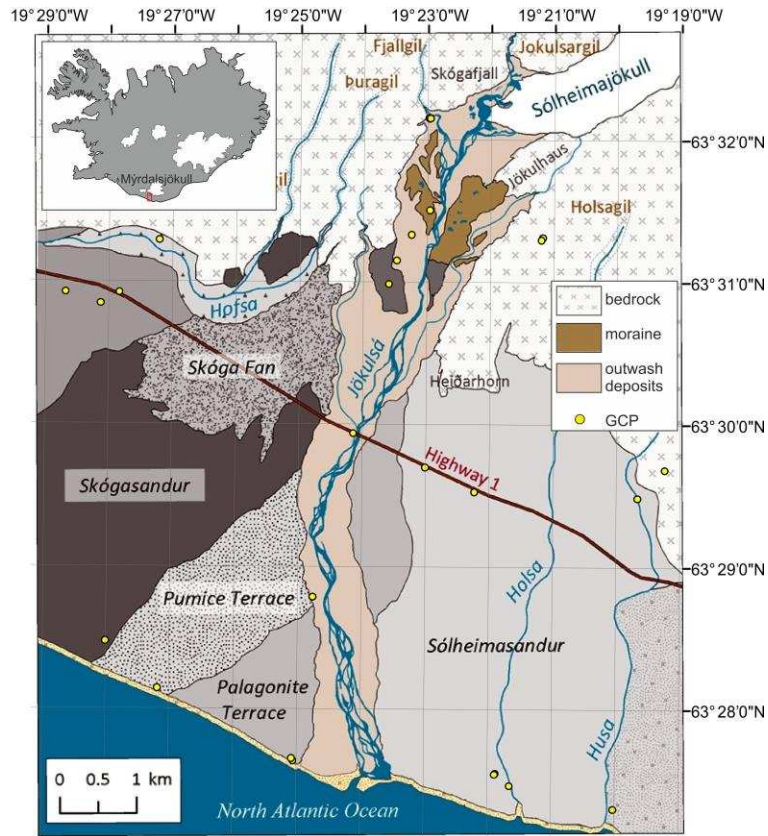
615 Table 3: Channel measurements in years from 1960 to 2010. Number of channel links measured at 114 cross-
616 sections spaced evenly between the glacier terminus and the Jökulsá estuary. Note the dramatic change between
617 1996 and 2001 coincident with the 1999 jökulhlaup and the switch from glacier terminus advance pre1996 to
618 retreat post-1996.

619

620

621 A multi-dimensional analysis of proglacial landscape
622 change at Sólheimajökull, southern Iceland

623 Kate E.H. Staines, Jonathan L. Carrivick, Fiona S. Tweed, Andrew J. Evans, Andrew J. Russell, Tómas
624 Jóhannesson, Matthew Roberts
625



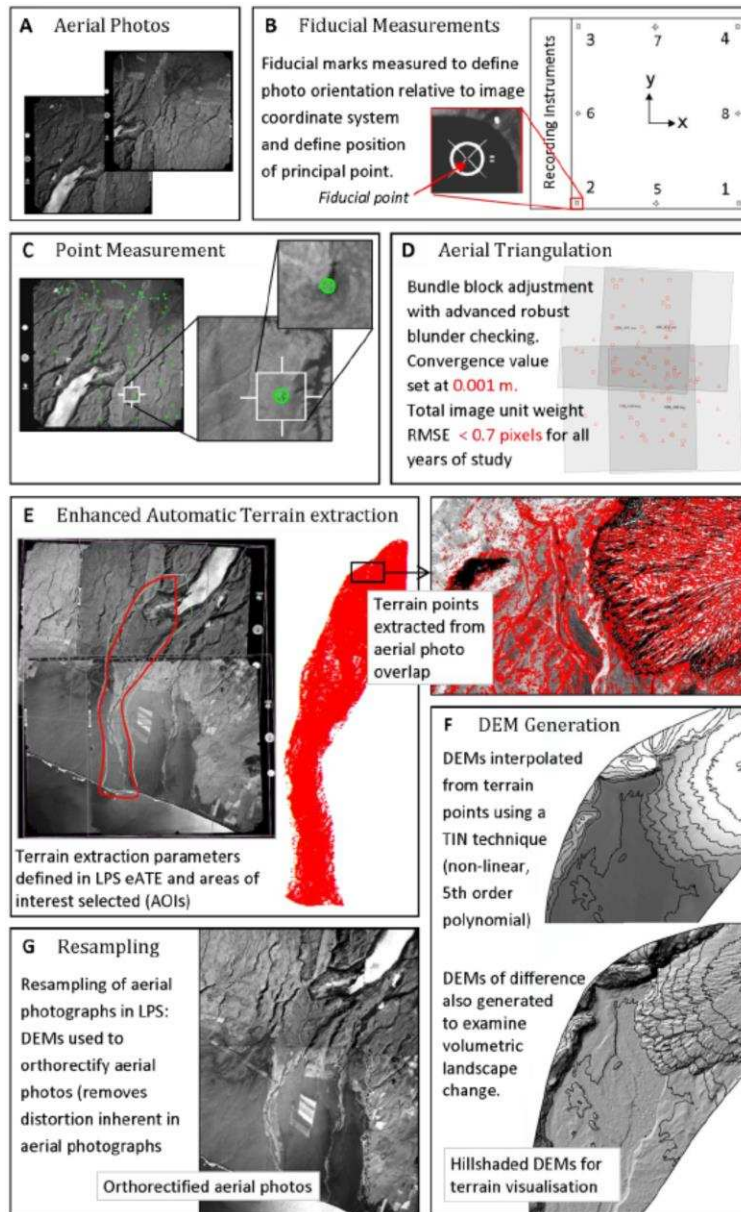
626
627

628 **Figure 1:** Overview of study site. The five distinct Holocene sandur surfaces (greyshades; named in italics) are
629 after Maizels (1989a, b). Note that 14 other GCPs were located outside of the limit of this diagram.

630
631
632
633
634

635 A multi-dimensional analysis of proglacial landscape
636 change at Sólheimajökull, southern Iceland

637 Kate E.H. Staines, Jonathan L. Carrivick, Fiona S. Tweed, Andrew J. Evans, Andrew J. Russell, Tómas
638 Jóhannesson, Matthew Roberts
639

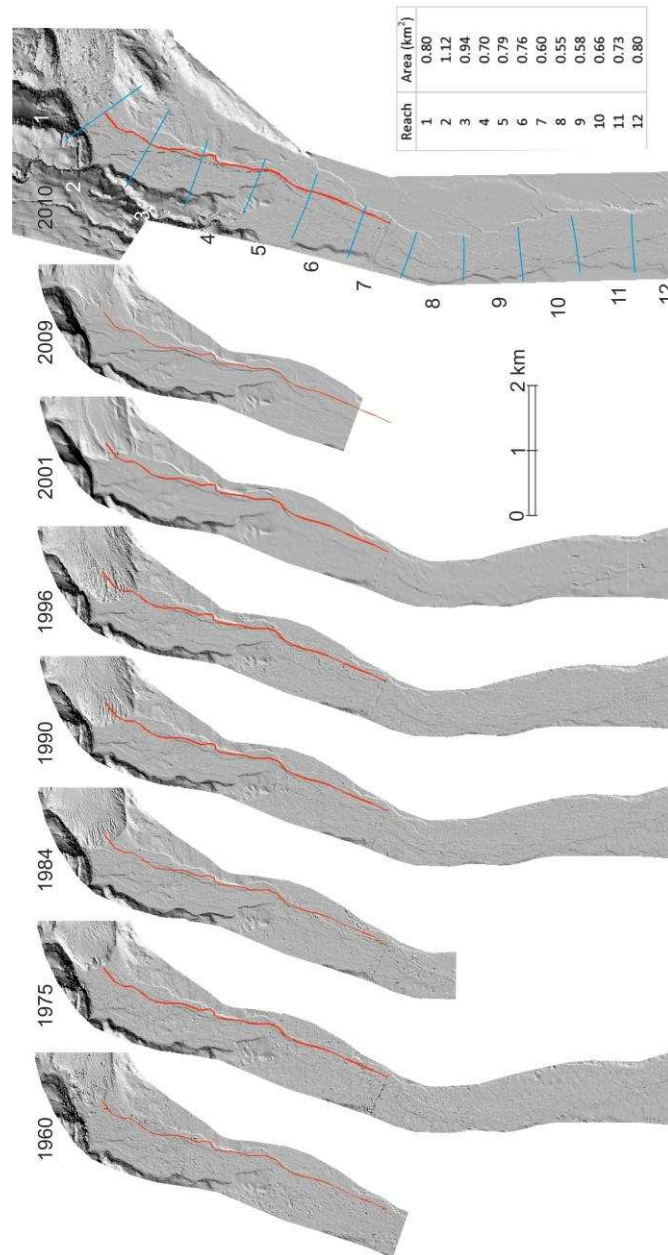


640
641 **Figure 2:** Overview of photogrammetry method used to create orthorectified images and to extract terrain.
642

643

644 A multi-dimensional analysis of proglacial landscape
645 change at Sólheimajökull, southern Iceland

646 Kate E.H. Staines, Jonathan L. Carrivick, Fiona S. Tweed, Andrew J. Evans, Andrew J. Russell, Tómas
647 Jóhannesson, Matthew Roberts



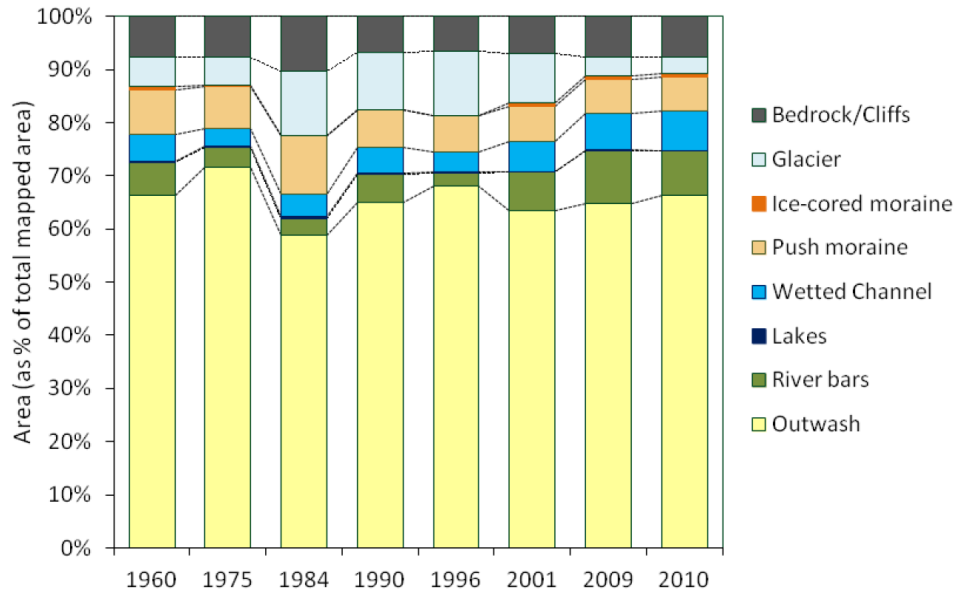
648

649 **Figure 3:** Hillshaded DEMs 1960 to 2010. DEMs 1960 to 1996 generated from photogrammetric terrain points.
650 2001 and 2009 DEMs created from contour lines. 2010 DEM created from airborne LiDAR point cloud. Definition
651 of fluvial reaches was based on mean wetted width. The red line is the long profile analysed in Figure 7. The inset
652 Table denotes the number and area of the 12 river reaches that are marked in the 2010 map, and that are used in
653 subsequent analysis of the river. A video animation of these hillshaded DEMs is provided as supplementary
654 information.

655

656 A multi-dimensional analysis of proglacial landscape
657 change at Sólheimajökull, southern Iceland

658 Kate E.H. Staines, Jonathan L. Carrivick, Fiona S. Tweed, Andrew J. Evans, Andrew J. Russell, Tómas
659 Jóhannesson, Matthew Roberts
660



661

662 **Figure 4.** Percentage area occupied by major categories of landforms. The 'glacier' refers only to the ice mapped
663 within the study area.
664

665

666

667

668

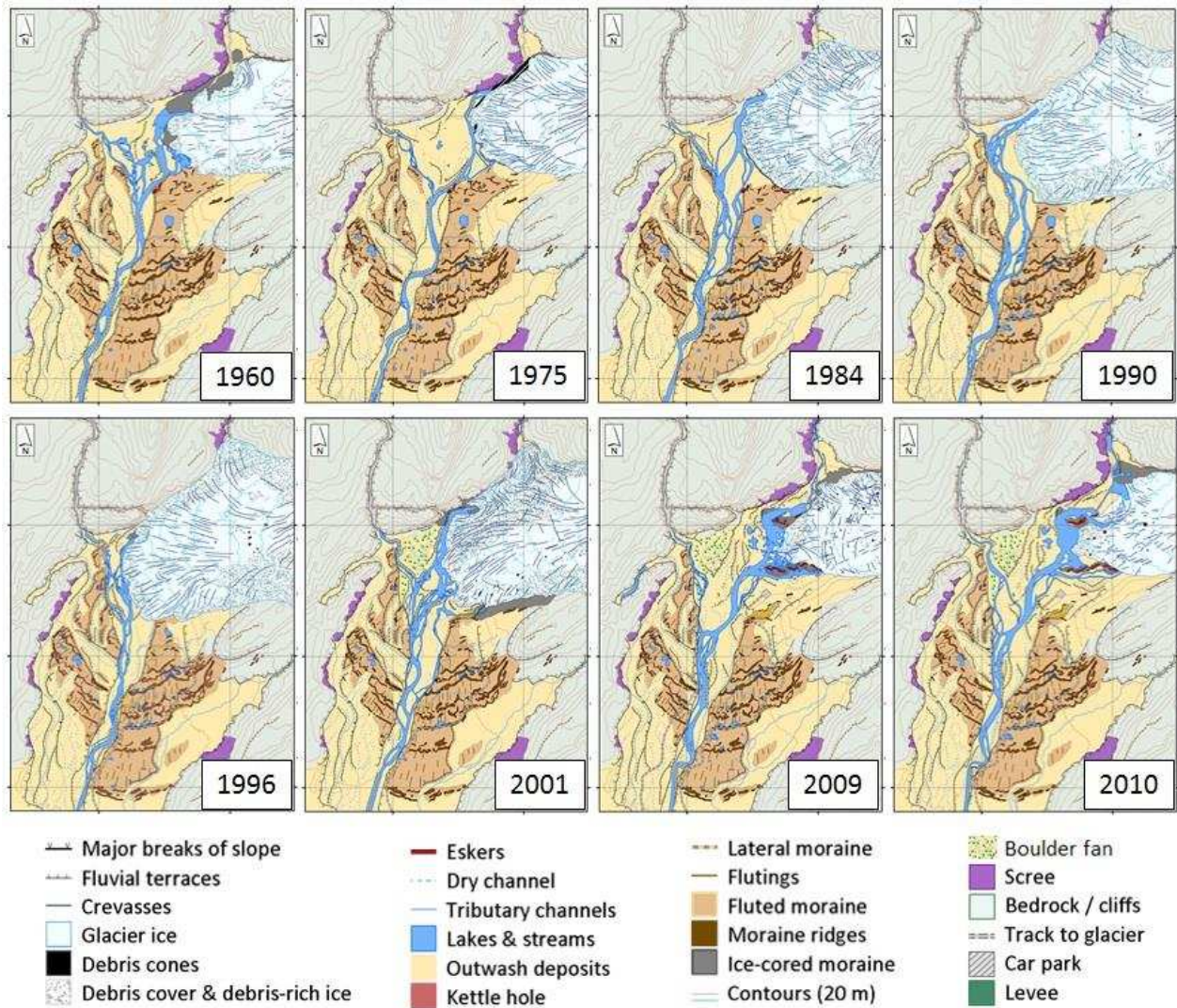
669

670

671

672 A multi-dimensional analysis of proglacial landscape
 673 change at Sólheimajökull, southern Iceland

674 Kate E.H. Staines, Jonathan L. Carrivick, Fiona S. Tweed, Andrew J. Evans, Andrew J. Russell, Tómas
 675 Jóhannesson, Matthew Roberts
 676

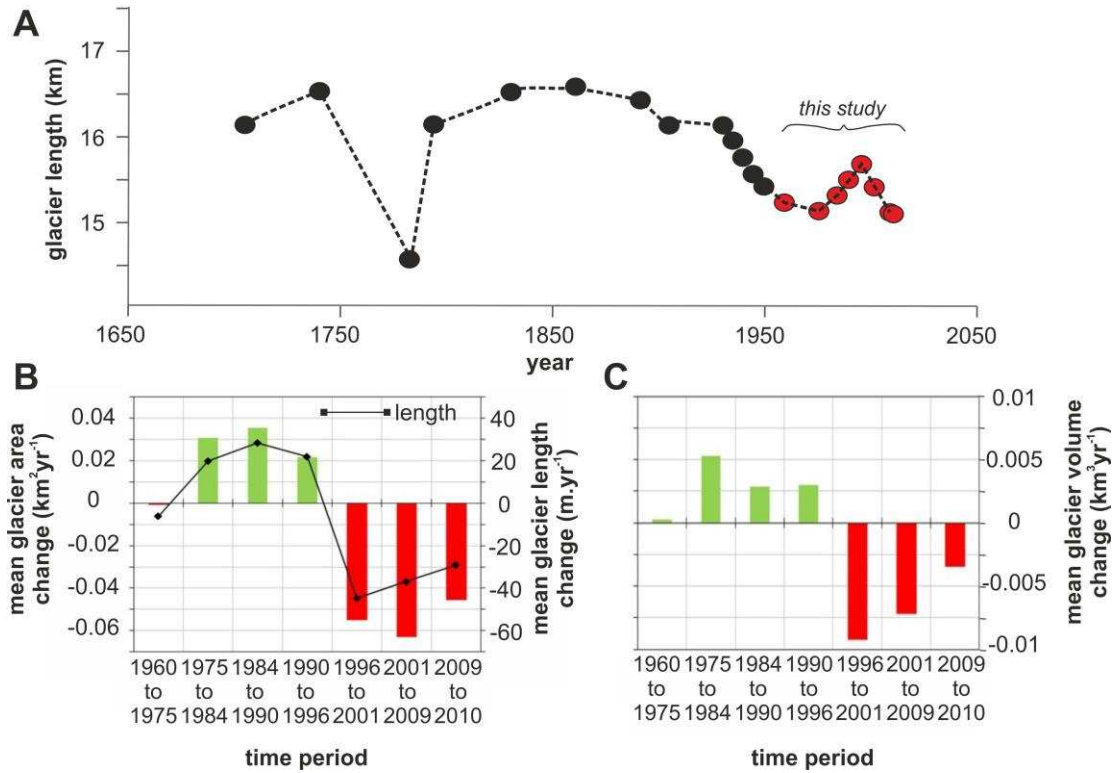


677
 678 **Figure 5:** Glacier and immediate ice-proximal area geomorphology from 1960 to 2010. A video animation of these
 679 maps is provided as supplementary information.

680

681 A multi-dimensional analysis of proglacial landscape
 682 change at Sólheimajökull, southern Iceland

683 Kate E.H. Staines, Jonathan L. Carrivick, Fiona S. Tweed, Andrew J. Evans, Andrew J. Russell, Tómas
 684 Jóhannesson, Matthew Roberts
 685



686
 687 **Figure 6:** Glacier length changes from data presented in Mackintosh (2002) and from this study (A), and mean
 688 annual rates of glacier area (bars) and length (line) (B), and volume (C) change.

689

690

691

692

693

694

695

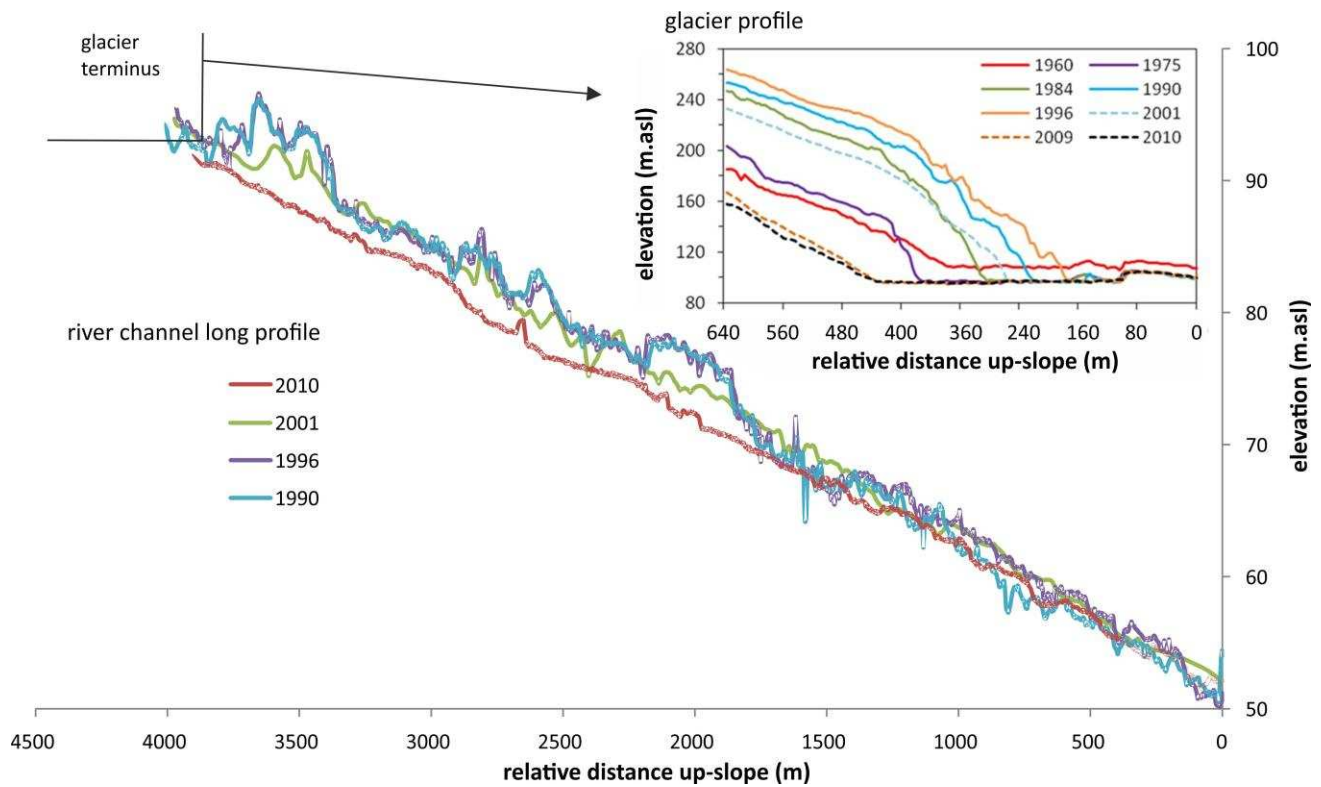
696

697 A multi-dimensional analysis of proglacial landscape
698 change at Sólheimajökull, southern Iceland

699 Kate E.H. Staines, Jonathan L. Carrivick, Fiona S. Tweed, Andrew J. Evans, Andrew J. Russell, Tómas
700 Jóhannesson, Matthew Roberts

701

702



703

704

705 **Figure 7:** Proglacial river long profile and glacier surface, for selected years. Note smoothing of river long profile
706 between 1996 and 2001 due to the 1999 jökulhlaup.

707

708

709

710

711

712

713

714

715

716

717

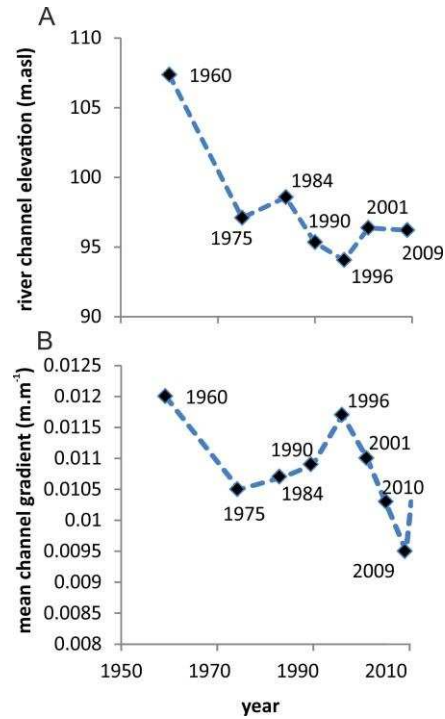
718

719

720 A multi-dimensional analysis of proglacial landscape
721 change at Sólheimajökull, southern Iceland

722 Kate E.H. Staines, Jonathan L. Carrivick, Fiona S. Tweed, Andrew J. Evans, Andrew J. Russell, Tómas
723 Jóhannesson, Matthew Roberts

724



725

726 **Figure 8:** Evolution of proglacial river channel head elevation (A) and mean gradient (B) in response to glacier
727 terminus position changes and ice-marginal lake development.

728

729

730

731

732

733

734

735

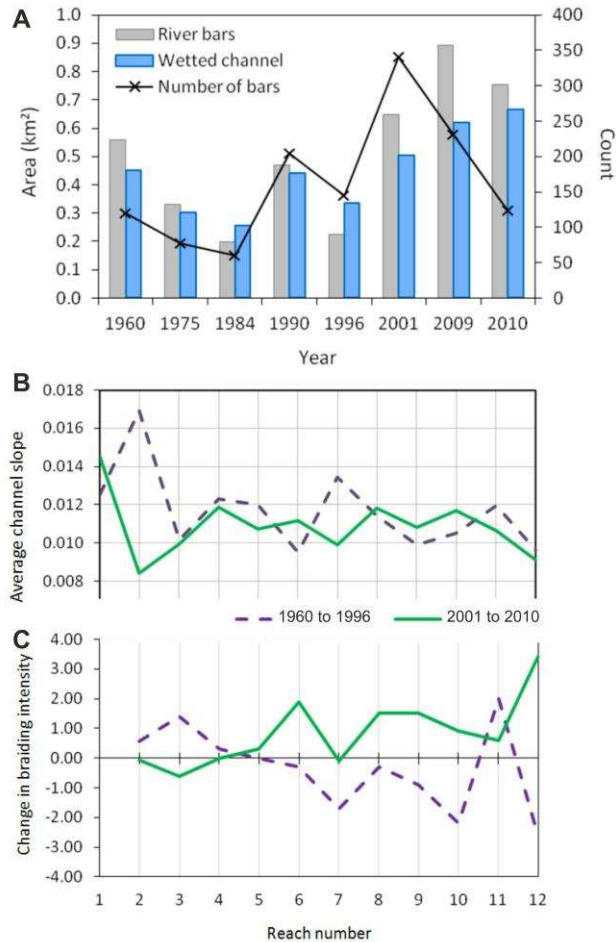
736

737 A multi-dimensional analysis of proglacial landscape
738 change at Sólheimajökull, southern Iceland

739 Kate E.H. Staines, Jonathan L. Carrivick, Fiona S. Tweed, Andrew J. Evans, Andrew J. Russell, Tómas
740 Jóhannesson, Matthew Roberts

741

742



743

744 **Figure 9:** Quantification of spatiotemporal evolution in proglacial braided river, using metrics of area of bars,
745 wetted area and number of bars (A), channel slope (B) and braiding intensity (C). Note highlighted difference in
746 the braided river in the time periods 1960 to 1996 and 2001 to 2010.

747

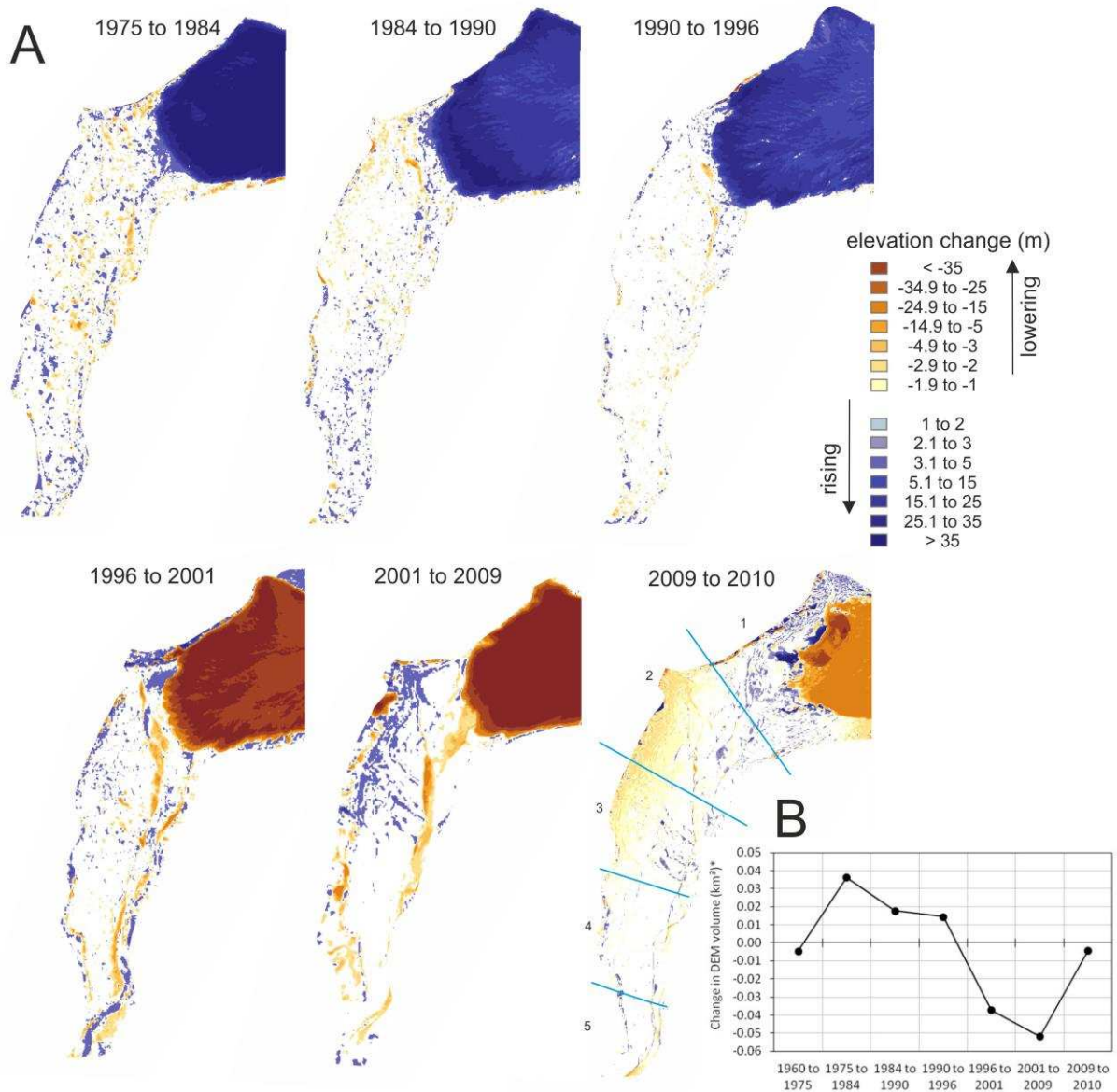
748

749

750

751 A multi-dimensional analysis of proglacial landscape
752 change at Sólheimajökull, southern Iceland

753 Kate E.H. Staines, Jonathan L. Carrivick, Fiona S. Tweed, Andrew J. Evans, Andrew J. Russell, Tómas
754 Jóhannesson, Matthew Roberts
755



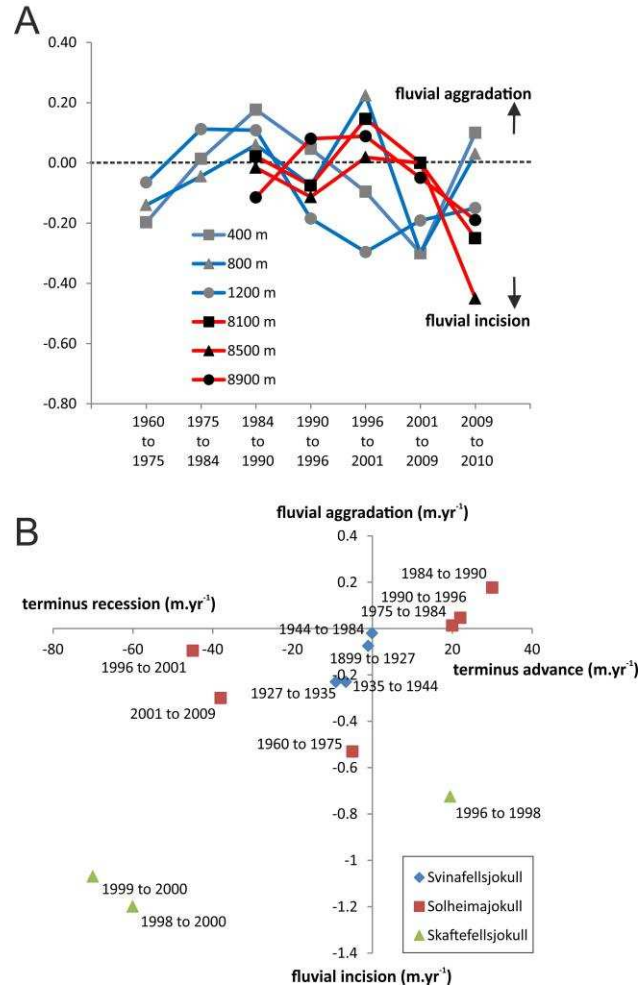
756

757 **Figure 10:** Spatial pattern of elevation changes in time periods between DEMs from 1960 to 2010 (A). Note glacier
758 advance and thickening until 1996, then recession of terminus and thinning. Note relative incoherence (which
759 includes some random error) in proglacial area up to 1996, then impact and adjustment to 1999 jökulhlaup. Part B
760 summarises the change in DEM volume for river reaches 1 to 6 (i.e. the most ice-proximal reaches) for each time
761 period.

762

763 A multi-dimensional analysis of proglacial landscape
 764 change at Sólheimajökull, southern Iceland

765 Kate E.H. Staines, Jonathan L. Carrivick, Fiona S. Tweed, Andrew J. Evans, Andrew J. Russell, Tómas
 766 Jóhannesson, Matthew Roberts
 767



768

769

770 **Figure 11:** Typical rates of elevation change in the proglacial fluvial area of Sólheimasandur, at three distances
 771 down channel from the ice margin chosen to be representative of proximal conditions (blue lines) and at three
 772 distances representing distal conditions (red lines) (A). Note data from just 6 of 114 cross sections are displayed in
 773 A for clarity. Part B illustrates a comparison of these mean rates of proglacial elevation change with data from
 774 Svinafellsjökull (Thompson and Jones, 1986) and Skatufellsjökull (Marren, 2002c). Note rates of change in
 775 elevation by all three studies in part B are based on elevation measurements at selected channel cross-sections;
 776 those from this study are those in part A. Note in part B the hint of a control of interval between observations on
 777 rates of elevation change measured.